View Online

Supramolecular metallomacrocycles based on *trans*-dicyanoferrite(III) building blocks: synthesis, crystal structure and magnetic properties†

Zhong-Hai Ni,[a] Jun Tao,[b] Wolfgang Wernsdorfer,[c] Ai-Li Cui[a] and Hui-Zhong Kou*[a]

Received 26th August 2008, Accepted 23rd January 2009
First published as an Advance Article on the web 23rd February 2009
DOI: 10.1039/b814860k

The reaction of *trans*-[Fe(R-bpb)$(CN)_2$]$^-$ (R-bpb^{2-} = R-substituted-1,2-bis(pyridine-2-carboxamido)benzenate) with *trans*-Mn(III) Schiff base complexes [Mn(5-X-saltn)]ClO_4 (5-X-saltn^{2-} = *N,N′*-propanolbis(5-X-substituted-salcylideneiminato) dianion) gave rise to cyanide-bridged neutral binuclear [MnFe] compounds [Mn(saltn)(MeOH)][Fe(bpb)$(CN)_2$]·3H_2O (**1**), [Mn(saltn)(H_2O)Fe-(bpmb)$(CN)_2$]·H_2O (**2**), [Mn(saltn)(MeOH)Fe(bpClb)$(CN)_2$]·2H_2O (**3**), and ionic [Mn_2Fe]$^+$-[Fe]$^-$ complexes [Mn_2(5-Br-saltn)$_2(H_2O)$(EtOH)Fe(bpb)$(CN)_2$][Fe(bpb)$(CN)_2$]·6H_2O (**4**) and [Mn_2(5-Cl-saltn)$_2(CH_3OH)$(EtOH)Fe(bpb)$(CN)_2$][Fe(bpb)$(CN)_2$]·5H_2O·MeCN (**5**). Four binuclear units of complexes **1–3** assemble in a head-to-tail way *via* hydrogen bonding giving rise to a metallo-supramolecular [MnFe]$_4$ square, while two [Mn_2Fe]$^+$-[Fe]$^-$ units of complexes **4–5** form a metallo-supramolecular macrocyclic structure. Magnetic studies reveal that complexes **1–3** and **5** exhibit intermetallic ferromagnetic coupling, while complex **4** displays antiferromagnetic interaction between low-spin Fe(III) and high-spin Mn(III) through the cyanide bridges. Complexes **1**, **4** and **5** display frequency dependent of current-alternating (ac) magnetic susceptibility, typical of the presence of slow magnetization relaxation. Because of the existence of intermolecular magnetic interaction, complex **4** shows an exchange-biased single-molecule magnet (SMM) behavior below 0.5 K.

Published on 23 February 2009 on http://pubs.rsc.org | doi:10.1039/B814860K
Downloaded by Xiamen University on 28 February 2011

Introduction

Single-molecule magnets (SMMs) have been an appealing theme in the field of molecular magnets because of their potential application in information storage and quantum computation.[1,2] SMMs are high-spin molecules with negative anisotropy, which generate an energy barrier between Ms and $-M$s. Slow relaxation of magnetization occurs near the blocking temperature (T_B) of the SMM. Below T_B, a hysteresis loop can be observed similar to the classical magnets. However, the magnetic properties of a SMM are greatly related to the intermolecular magnetic interaction.[3] In fact, it is difficult to completely remove the intermolecular magnetic coupling, and what we can do is to make the unwanted interaction the least. Therefore, the studies on the intermolecular magnetic interaction are important, and SMM-based polynuclear or polymeric compounds are suitable targets.[3]

Recently, we employed the dicyano-containing building block *trans*-[Fe(bpb)$(CN)_2$]$^-$ (bpb^{2-} = 1,2-bis(pyridine-2-carboxamido)benzenate) to synthesize polynuclear complexes with the hope of finding new SMMs.[4] Interestingly, we have found that the reaction of the Schiff base complex [Mn(salen)]ClO_4 with the *R*-substituted bpb^{2-} precursor [Fe(R-bpb)$(CN)_2$]$^-$ (Scheme 1) gave a unique cyanide-bridged Mn_6Fe_6 molecular wheel that shows SMM behavior.[5] It indicates that *trans*-[M(L)$(CN)_2$]$^-$ is able to construct high-nuclearity molecules. Nevertheless, two equivalence building blocks with two donors and acceptors at the *trans* positions frequently form alternate 1D Mn^{III}–Fe^{III} chain structures.[4] In order to find a route to prepare polynuclear Mn^{III}(Schiff base)–Fe^{III}(bpb)$(CN)_2$ complexes, we modified the Schiff base around Mn(III), *i.e.* using [Mn(5-X-saltn)]$^+$ (Scheme 1) instead of [Mn(salen)]$^+$. The flexibility of the trimethylene group in 5-X-saltn^{2-} should induce the pucker of the Schiff base ligand, which hinders the coordination of the cyano nitrogen atom because of steric constraints. Thus, cyanide-bridged di- or tri-nuclear complexes are expected to form instead of the usual one-dimensional species.[5] Further supramolecular assembly of the polynuclear units provides species for studies on the effect of intermolecular magnetic interaction. We report here the synthesis,

[a]*Department of Chemistry, Tsinghua University, Beijing, 100084, P. R. China. E-mail: kouhz@mail.tsinghua.edu.cn; Fax: 86 10–6277 1748; Tel: 86 10–6277 1748*
[b]*Department of Chemistry, State Key Laboratory for Physical Chemistry of Solid Surfaces, Xiamen University, Xiamen, 361005, P. R. China*
[c]*Laboratoire Louis Néel-CNRS, 38042, Grenoble, Cedex 9, France*

† Electronic supplementary information (ESI) available: Important hydrogen bonding interaction in complexes **1–5**. Crystal structures of complexes **2**, **3** and **5**. Cell packing diagrams for complexes **1–5**. Field dependence of magnetization of complex **5** at 2 K. Hysteresis loop for complex **4** at different temperatures measured at the constant scan magnetic field speed of 0.14 T s^{-1}. CCDC reference numbers 651026–699873. For ESI and crystallographic data in CIF or other electronic format see DOI: 10.1039/b814860k

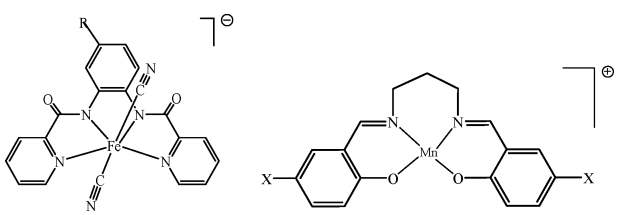

Scheme 1 Structures of building blocks [Fe^{III}(R-bpb)$(CN)_2$]$^-$ (R-bpb^{2-} = bpb^{2-} (R = H), bpmb^{2-} (R = CH_3), bpClb^{2-} (R = Cl), and [Mn^{III}(5-X-saltn)]$^+$ (5-X-saltn = saltn^{2-} (X = H), 5-Clsaltn^{2-} (X = Cl), 5-Brsaltn^{2-} (X = Br)) used for the synthesis.

 This journal is © The Royal Society of Chemistry 2009

View Online

Published on 23 February 2009 on http://pubs.rsc.org | doi:10.1039/B814860K
Downloaded by Xiamen University on 28 February 2011

structure and magnetic properties of five bimetallic Mn(III)–Fe(III) complexes based on this strategy.

Experimental

Materials

All the chemicals were of AR grade and used as received. K[Fe(R-bpb)(CN)$_2$][6,7] and [Mn(5-X-saltn)]ClO$_4$[8] were synthesized according to a literature method.

Physical measurements

Elemental analyses (C, H, N) were carried out with an Elementar Vario EL analyzer. IR spectra were recorded on a Nicolet Magna-IR 750 spectrometer in the 4000–650 cm^{-1} region. Temperature- and field-dependent magnetic susceptibility measurements were carried out on a Quantum Design SQUID magnetometer. The alternating-current (ac) magnetic susceptibility measurements were performed on a MagLab 2000 magnetometer. The experimental susceptibilities were corrected for the diamagnetism of the constituent atoms (Pascal's Tables).

Single crystal X-ray data of **1–5** were collected on a Siemens Bruker P4, Rigaku R-AXIS RAPID IP or a Saturn 70 CCD diffractometer. The structures were solved by direct method SHELXS-97 and refined by full-matrix least-squares (SHELXL-97) on F^2. Hydrogen atoms were added geometrically and refined using a riding model. The crystals are either twin or weakly diffract, giving heavy disorder of some atoms and high $R1$ values for complexes **4** and **5**.

Synthesis

Synthesis of complexes 1–3. The synthesis of complexes **1–3** is similar, and only the synthetic procedure for complex **1** is given in detail. To a solution of K[Fe(bpb)(CN)$_2$] (69.2 mg, 0.15 mmol) in MeOH/H$_2$O (5 mL, 4:1 v/v) was added [Mn(saltn)]ClO$_4$ (65.4 mg, 0.15 mmol) in MeOH/MeCN (6 mL, 2:1 v/v). The brown mixture was immediately filtered and then left to stand undisturbed for evaporation at room temperature. Well-shaped parallelogram dark brown single crystals suited for X-ray diffraction measurement were obtained. Yield: *ca.* 40%. Elemental analysis (%): calcd for $C_{38}H_{34}FeMnN_8O_6$ (**1**): C 56.38, H 4.23, N 13.84; Found: C 56.52, H 4.68, N 13.95. IR(KBr, cm^{-1}): 2127.

Elemental analysis (%) for complex **2**: calcd for $C_{38}H_{34}FeMnN_8O_6$: C 56.38, H 4.23, N 13.84; Found: C 56.05, H 4.67, N 13.65. IR(KBr, cm^{-1}): 2128. Yield: 50%.

Elemental analysis (%) for complex **3**: calcd for $C_{38}H_{33}ClFeMnN_8O_6$: C 54.08, H 3.94, N 13.28; Found: C 52.95, H 4.09, N 13.00. IR(KBr, cm^{-1}): 2127. Yield: 60%.

Synthesis of complexes 4 and 5. Complex **4** was prepared by slow diffusion of equimolar [Mn(5-Br-saltn)]ClO$_4$ (0.1 mmol, MeOH-EtOH-CH$_3$CN, 2:1:1 v/v/v) and K[Fe(bpb)(CN)$_2$] (0.1 mmol, MeOH-EtOH-H$_2$O, 4:2:1 v/v/v) in a single tube. Good-quality, black single crystals were obtained after one week which are subjected to X-ray diffraction analysis. Yield: *ca.* 50%. Elemental analysis (%): calcd for $C_{76}H_{72}Br_4Fe_2Mn_2N_{16}O_{16}$ (**4**): C 45.49, H 3.62, N 11.17; Found: C 45.08, H 3.88, N 10.92. IR(KBr, cm^{-1}): 2121.

Complex **5** was synthesized in a way similar to complex **4** using [Mn(5-Cl-saltn)]ClO$_4$ instead. Yield: *ca.* 55%. Elemental analysis (%): calcd for $C_{79}H_{77}Cl_4Fe_2Mn_2N_{17}O_{16}$ (**4**): C 50.37, H 4.12, N 12.64; Found: C 50.36, H 3.96, N 13.02. IR(KBr, cm^{-1}): 2123.

Results and discussion

Structural descriptions

Crystal data and structure refinement details for compounds **1**, **4** and **5** are listed in Table 1. Important structural parameters are collected in Tables 2 and 3. The structural diagrams are shown in Fig. 1 and 2, while the figures for cell packing are given in the ESI.†

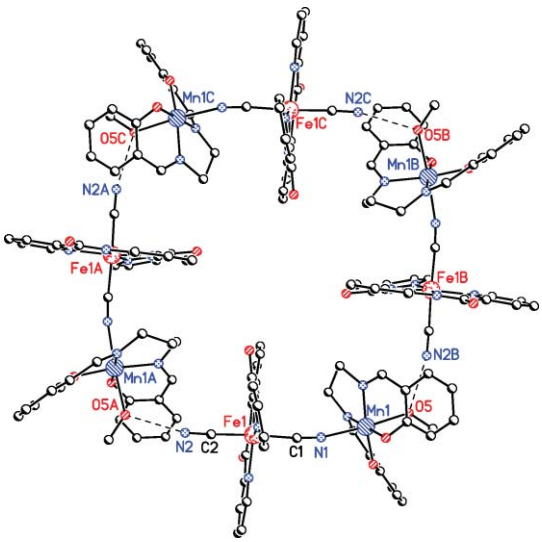

Fig. 1 Structure of a supramolecular square formed from four dinuclear MnFe units of complex **1**. Hydrogen atoms are omitted for clarity.

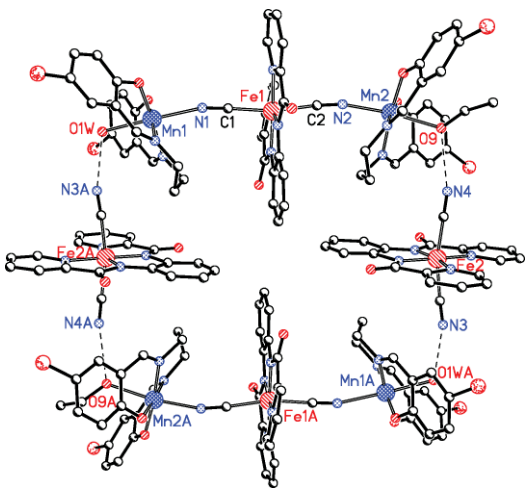

Fig. 2 Structure of a supramolecular macrocycle for complex **4**.

Compounds **1–3** are iso-structural and consist of a cyanide-bridged neutral FeMn dinuclear structure (Fig. 1 and Fig. S1–2†). Because of the low quality of the crystal data for compounds **2** and **3**, the data were given as ESI† for reference. The

View Online

Published on 23 February 2009 on http://pubs.rsc.org | doi:10.1039/B814860K
Downloaded by Xiamen University on 28 February 2011

Table 1 Crystallographic data for complexes **1**, **4** and **5**

	1	**4**	**5**
formula	$C_{38}H_{34}FeMnN_8O_6$	$C_{76}H_{72}Br_4Fe_2Mn_2N_{16}O_{16}$	$C_{79}H_{77}Cl_4Fe_2Mn_2N_{17}O_{16}$
Fw	809.52	2006.72	1883.96
T/K	293(2)	297(2)	123(2)
crystal system	tetragonal	triclinic	triclinic
space group	$P\text{-}42_1c$	$P\text{-}1$	$P\text{-}1$
a/Å	23.065(3)	15.960(4)	15.771(6)
b/Å	23.065(3)	15.992(5)	15.849(5)
c/Å	15.363(5)	18.327(5)	18.403(6)
α/deg	90	73.085(6)	77.540(16)
β/deg	90	77.852(5)	73.189(15)
γ/deg	90	79.133(6)	78.680(16)
V/Å^3	8174(3)	4334(2)	4255(3)
Z	8	2	2
ρ_{calcd}/g cm^{-1}	1.316	1.538	1.470
F(000)	3336	2020	1936
Reflections collected	9187	23705	28582
R*int*	0.0258	0.1379	0.0961
Reflections [$I > 2\sigma(I)$]	3966	4282	8568
Goodness-of-fit on F^2	1.011	1.064	1.084
data/restraints/params	4545/9/505	15027/12/1045	14706/14/1091
R1[$I > 2\sigma$(I)]	0.0582	0.1015	0.1081
wR2(all data)	0.1735	0.3351	0.2869
Largest diff. peak, hole (e Å^{-3})	0.896, –0.502	0.925, –0.506	1.237, –0.856
CCDC number	699870	651026	699873

Table 2 Selected bond distances (Å) and bond angles (°) for complex **1**

Mn(1)–N(1)	2.256(3)	Mn(1)–N(7)	2.050(3)
Mn(1)–N(8)	2.025(3)	Mn(1)–O(3)	1.878(2)
Mn(1)–O(4)	1.892(3)	Mn(1)–O(5)/O(1 W)	2.310(2)
Fe(1)–C(1)	1.979(3)	Fe(1)–C(2)	1.943(3)
Fe(1)–Mn(1)	5.306(2)	Fe(1)–Mn(1)′	7.013(2)
Mn(1)–N(1)–C(1)	167.4(3)		

Table 3 Selected bond distances (Å) and bond angles (°) for complexes **4** and **5**

	4	**5**
Mn(1)–N(1)	2.252(16)	2.251(7)
Mn(1)–O(1 W)/O(10)	2.229(11)	2.251(6)
Mn(2)–N(2)	2.154(14)	2.207(7)
Mn(2)–O(9)	2.291(11)	2.291(6)
Fe(1)–C(1)	1.953(19)	1.971(9)
Fe(1)–C(2)	1.966(17)	1.956(9)
Fe(1)–Mn(1)	5.282(3)	5.324(2)
Fe(1)–Mn(2)	5.191(3)	5.229(2)
Mn(1)–N(1)–C(1)	166.6(13)	166.7(6)
Mn(2)–N(2)–C(2)	162.7(12)	158.3(7)

Mn(III) ion exhibits an axially elongated octahedral configuration, which is equatorially coordinated by two nitrogen atoms and two phenoxo oxygen atoms of saltn^{2-}, and axially linked to one methanol/ethanol/water oxygen atom and a cyanide nitrogen atom of [Fe(R-bpb)(CN)$_2$]$^-$ moiety. The bridging Mn–N≡C bond angle deviates slightly from linearity, 167.4(3)° for complex **1**. The intramolecular Mn–Fe separation is 5.306(2) Å.

Four dinuclear units are linked head-to-tail by hydrogen bonding between the non-bridging cyano nitrogen atoms and the coordinating methanol/ethanol oxygen atoms, giving rise to a supramolecular square. The length of the each side of the square for complex **1** is *ca.* 14.8 Å. Because of the *trans*-configuration of the building blocks in complexes **1–3** it is impossible to form cyanide-linked Mn_2Fe_2 or Mn_4Fe_4 squares, and only Mn_6Fe_6 wheels can be generated.[4,5] The lattice water molecules are situated at the vicinity of the clusters, and are linked to the supramolecular macrocycles (ESI, Fig. S4†).

Complexes **4** and **5** are isostructural, and the structure of complex **4** is only described in detail. The structure of **4** consists of a cyanide-bridged trinuclear [Mn$_2$(5-Br-saltn)$_2$(EtOH)(H$_2$O)(μ-CN)$_2$Fe(bpb)]$^+$ cation and a free [Fe(bpb)(CN)$_2$]$^-$ anion (Fig. 2). In the trinuclear cation, [Fe(bpb)(CN)$_2$]$^-$ uses two *trans*-cyanide ligands to connect two [Mn(5-Br-saltn)]$^+$, resulting in a linear Mn–Fe–Mn arrangement. The C≡N–Mn bond angles are a little different: 166.6(13)° for C(1)–N(1)–Mn(1) and 162.7(12)° for C(2)–N(2)–Mn(2). The Mn–N$_{cyano}$ bond distances are 2.252(16) Å for Mn(1)–N(1) and 2.154(14) Å for Mn(2)–N(2). The Mn–Fe separations through the cyanide bridges are 5.282(3) Å (Mn(1)–Fe(1)) and 5.191(3) Å (Mn(2)–Fe(1)), respectively. The Mn(III) ions have elongated octahedral coordination with the solvent EtOH or H$_2$O oxygen atom occupying the axial position *trans* to the cyano nitrogen atom. The equatorial sites are taken by the atoms of the 5-Br-saltn^{2-} ligand. As expected, the benzene groups deviate greatly from the N$_2$O$_2$ plane forming a puckered configuration (Fig. 2).

The trinuclear cations and free [Fe(bpb)(CN)$_2$]$^-$ anions are not isolated but are connected by N$_{cyano}$–H–O hydrogen bonding (broken lines in Fig. 2). The N$_{cyano}$–O separations are 2.835(17) Å for O(9)–N(4) and 2.724(19) Å for O(1 W)–N(3#2) (Table 4). Therefore, a novel supramolecular macrocycle is formed. There is a weak π–π interaction between the benzene rings of non-bridging [Fe(bpb)(CN)$_2$]$^-$ from adjacent macrocycles, yielding a 2D layered structure (ESI†). The Fe–Fe separation through the π–π contacts is 6.395(1) Å, even shorter than the intra-macrocycle Mn–Fe distance (6.636(1) Å).

 This journal is © The Royal Society of Chemistry 2009

View Online

Published on 23 February 2009 on http://pubs.rsc.org | doi:10.1039/B814860K
Downloaded by Xiamen University on 28 February 2011

Table 4 Hydrogen bonding interaction within the supramolecular clusters in complexes **1**, **4** and **5**

	D–H	d(D–H)	d(H···A)	∠DHA	d(D···A)	A
1	O5-H5	0.890	1.927	172.28	2.812(3)	N2#1
4	O1W–H1WB	0.856	1.867	179.36	2.724(19)	N3#2
	O9-H9A	0.867	1.989	164.07	2.835(17)	N4
5	O9-H9A	0.850	1.967	163.94	2.793(4)	N3
	O10-H10A	0.853	1.887	166.69	2.725(4)	N4#3

Symmetry operations: #1 –y, x, –z; #2 -x + 2, –y, -z + 1; #3 -x + 1, –y + 1, –z.

Magnetic properties

Variable-temperature magnetic susceptibilities of complexes **1–5** have been measured on a MagLab 2000 or a SQUID magnetometer in an applied magnetic field of 1 kOe. Fig. 3–6 show the $\chi_m T$ *vs.* T plots for complexes **1–5**, respectively.

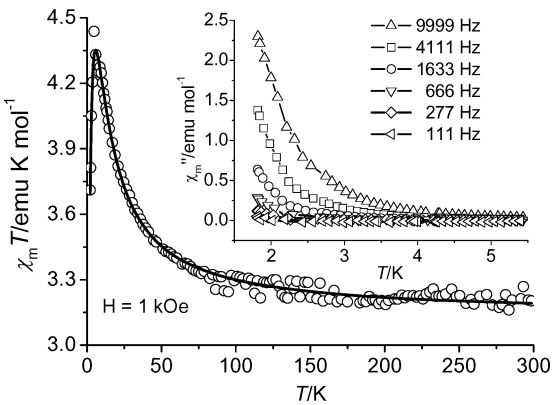

Fig. 3 Temperature dependence of $\chi_m T$ per MnFe for complex **1**. The line represents the best fit using the parameters discussed in the text. Inset: out-of-phase ac magnetic susceptibilities of **1** measured under zero dc magnetic field.

Magnetic properties of complex 1. The $\chi_m T$ product per MnFe is equal to 3.2 emu K mol^{-1} at 300 K, slightly lower than the spin-only value of 3.375 emu K mol^{-1} for a high-spin Mn(III) ion ($S = 2$) and one low-spin Fe(III) ion ($S = 1/2$) with $g = 2.0$. With the decrease of the temperature, $\chi_m T$ increases gradually reaching the maximum value of 4.4 emu K mol^{-1} at 4.8 K. Below 4.8 K, $\chi_m T$ rapidly decreases, and attains 3.7 emu K mol^{-1} at 2 K. This magnetic behavior suggests the presence of global ferromagnetic interaction with the cooperation of zfs of Mn(III) and/or intermolecular magnetic coupling.

To evaluate the strength of intra-/inter-dimer magnetic coupling (J/zJ') and zfs parameter (D) of Mn(III), equation (1)[9] based on $\hat{H} = -2J\hat{S}_{Mn}\cdot\hat{S}_{Fe} + D_{Mn}(\hat{S}_z^2 - \frac{S_{Mn}(S_{Mn}+1)}{3}) + g\beta H\hat{S} - zJ'\langle S_z^T\rangle\hat{S}_z^T$ has been used to fit the experimental magnetic data, giving the fitting parameters of $J = 3.2(1)$ cm^{-1}, $g = 1.93(1)$, $D_{Mn} = 1.25(3)$ cm^{-1}, $zJ' = -0.15(1)$ cm^{-1}, and $R = (\Sigma(\chi_{calc}T - \chi_{obsd}T)^2)/\Sigma(\chi_{obsd}T)^2 = 3.8\times10^{-6}$. It should be mentioned that both positive and negative D_{Mn} values give a satisfactory fit, and therefore based on the powder magnetic susceptibility data it is difficult to determine the sign of D_{Mn}. The calculated D_{Mn} value (1.25 cm^{-1}) is normal for high-spin tetragonally elongated octahedral Mn(III). In addition,

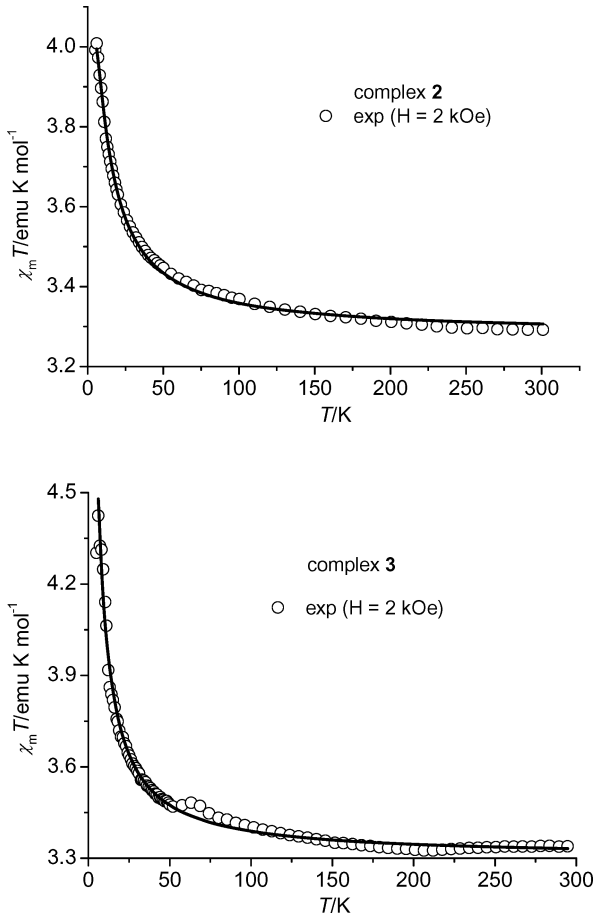

Fig. 4 Temperature dependence of $\chi_m T$ per MnFe for complexes **2** and **3**. The line represents the best fit in the temperature range 6–300 K.

D_{Mn} and zJ' are often correlated, and they should be treated with care.

$$\chi_{dinuclear} = \frac{Ng^2\beta^2}{4kT}\left[\frac{25\exp(A)+9\exp(B)+\exp(C)+9\exp(G)+\exp(E)}{\exp(A)+\exp(B)+\exp(C)+\exp(G)+\exp(E)}\right]$$

$$A = \left(\frac{35J}{4}+4D\right)/kT,\ B = \left[\frac{25}{4}J+\frac{5D}{2}+\left(\frac{25}{4}J^2-\frac{9}{2}DJ+\frac{9}{4}D^2\right)^{\frac{1}{2}}\right]/kT,$$

$$C = \left[\frac{25}{4}J+\frac{D}{2}+\left(\frac{25}{4}J^2-\frac{1}{2}DJ+\frac{1}{4}D^2\right)^{\frac{1}{2}}\right]/kT,$$

$$G = \left[\frac{25}{4}J+\frac{5D}{2}-\left(\frac{25}{4}J^2-\frac{9}{2}DJ+\frac{9}{4}D^2\right)^{\frac{1}{2}}\right]/kT,$$

$$E = \left[\frac{25}{4}J+\frac{D}{2}-\left(\frac{25}{4}J^2-\frac{1}{2}DJ+\frac{1}{4}D^2\right)^{\frac{1}{2}}\right]/kT,$$

$$\chi_m = \frac{\chi_{dinuclear}}{1-2zJ'\chi_{dinuclear}/Ng^2\beta^2} \quad (1)$$

The alternating-current (ac) magnetic susceptibility measurements for complex **1** were performed in a 3 G ac field oscillating at 111–9999 Hz, with a zero dc magnetic field, on the polycrystalline samples (inset of Fig. 3). Complex **1** exhibits obvious frequency-dependent χ_m'' signals at $T < 3$ K, suggesting the presence of slow relaxation of magnetization. The absence of a maximum down to 1.8 K precludes any further characterization of the magnetization relaxation.

View Online

Published on 23 February 2009 on http://pubs.rsc.org | doi:10.1039/B814860K
Downloaded by Xiamen University on 28 February 2011

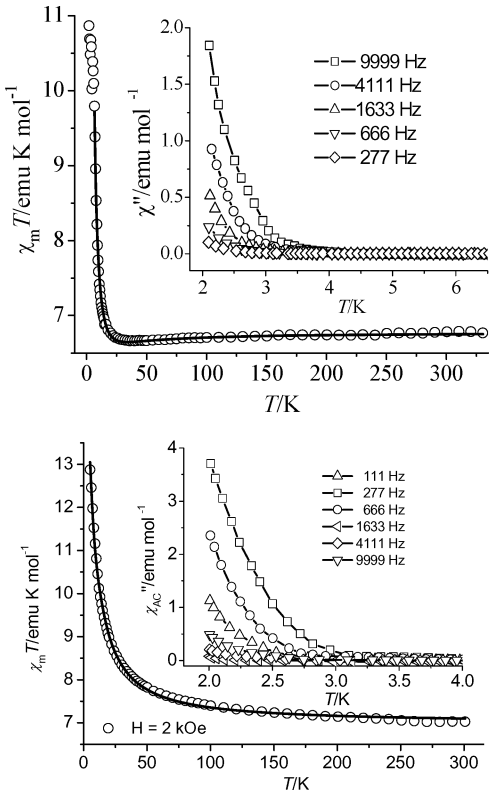

Fig. 5 Temperature dependence of $\chi_m T$/Mn_2Fe_2 for complexes **4** (top) and **5** (bottom). The line represents the best fit using the parameters discussed in the text. Inset: out-of-phase ac magnetic susceptibilities measured under zero dc magnetic field.

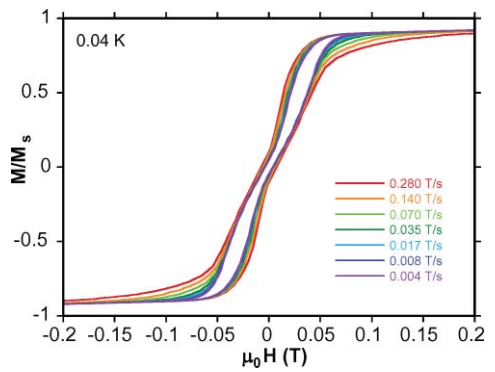

Fig. 6 Hysteresis loop for complex **4** at 0.04 K.

Magnetic properties of complexes 2 and 3. Temperature dependence of $\chi_m T$ per MnFe for complexes **2** and **3** is shown in Fig. 4. The room-temperature $\chi_m T$ value is 3.29 emu K mol^{-1} (complex **2**) and 3.33 emu K mol^{-1} (complex **3**), close to the spin-only value of 3.375 emu K mol^{-1} for a high-spin Mn(III) ion (S = 2) and a low-spin Fe(III) ion (S = 1/2) with g = 2.0. The $\chi_m T$ value gradually increases with the decrease of the temperature, reaching the maximum value of 4.0 emu K mol^{-1} (complex **2**) and 4.42 emu K mol^{-1} (complex **3**) at 6 K. Whereafter, $\chi_m T$ decreases, amounting to 3.99 emu K mol^{-1} K (complex **2**) and 4.30 emu K mol^{-1} (complex **3**) at 5 K. This magnetic behavior is indicative of the presence of Fe(III)–Mn(III) ferromagnetic coupling through the cyanide bridge. The decrease of $\chi_m T$ below 6 K may be due to the zfs of Mn(III) and/or the intermolecular magnetic interaction.

The use of four parameters (J, D, zJ' and g) in eqn (1) to fit the magnetic susceptibilities of complexes **2** and **3** failed. Therefore, D or zJ' was exclusively used for the fitting. The value of one parameter should contain the contribution of another one. The satisfactory fitting results, in the temperature range 6–300 K, are shown as solid red lines in Fig. 4, and the fit parameters are: J = 2.06(4) cm^{-1}, g = 1.97(1) cm^{-1}, D = –0.10(1) cm^{-1}, and $R = (\Sigma(\chi_{calc}T-\chi_{obsd}T)^2)/\Sigma(\chi_{obsd}T)^2 = 1.30\times10^{-4}$ for complex **2**, and J = 1.56(8) cm^{-1}, g = 1.98(1) cm^{-1}, D = 0.35(3) cm^{-1}, and $R = 1.44\times10^{-4}$ for complex **3**. Using zJ' instead of D gave a similar fitting result with the parameters J = 2.04(4) cm^{-1}, g = 1.97(1) cm^{-1}, zJ' = –0.023(2) cm^{-1}, and $R = 1.28\times10^{-4}$ for complex **2**, and J = 1.71(6) cm^{-1}, g = 1.98(1) cm^{-1}, zJ' = 0.068(4) cm^{-1}, and $R = 1.42\times10^{-4}$ for complex **3**. It is strange that the zJ' value for complex **2** is negative, which indicates the presence of an intermolecular antiferromagnetic interaction. Basically, the zJ' value contains the contribution of zfs of Mn(III), intra- and inter-cluster (Mn_4Fe_4) magnetic coupling. Therefore, we cannot assume unambiguously that the intra-cluster magnetic coupling through H-bonding is antiferromagnetic on the basis of this fitting result.

Magnetic properties of complexes 4 and 5. Temperature dependence of magnetic susceptibilities in the form of $\chi_m T$ per Mn_2Fe_2 has been measured in an applied magnetic field of 1 kOe (complex **4**) and 2 kOe (complex **5**) on a SQUID magnetometer (Fig. 5). The room temperature $\chi_m T$ value is 6.76 emu K mol^{-1} (complex **4**) and 7.02 emu K mol^{-1} (complex **5**), close to the spin-only value of 6.75 emu K mol^{-1} for an uncoupled $Mn_2^{III}Fe_2^{III}$ system with g = 2.0. The constant decrease of $\chi_m T$ with the decrease of temperature for complex **4** suggests the presence of dominant antiferromagnetic Mn^{III}–Fe^{III} coupling through the cyanide bridges. The abrupt increase below 40 K is due to the presence of the net spins of antiparallel S_{Mn} and S_{Fe} within the trinuclear cations, giving rise to a ground spin state of $S = 2\times S_{Mn} - S_{Fe} = 2\times2-1/2 = 7/2$. There is no decrease in $\chi_m T$ until 2 K, indicating that the intermolecular magnetic interaction is likely to be ferromagnetic.

The magnetic behavior of complex **5** is different from that of complex **4**. On lowering the temperature, the $\chi_m T$ value of complex **5** gradually increases and reaches a value of 12.87 emu K mol^{-1} at 5 K. This magnetic behavior indicates the presence of overall ferromagnetic interactions in complex **5**.

To evaluate the strength of Mn(III)–Fe(III) magnetic coupling *via* the cyanide bridges, the equation (ESI†) based on the isotropic Hamiltonian $\hat{H} = -2J(\hat{S}_{Fe1}\hat{S}_{Mn1} + \hat{S}_{Fe1}\hat{S}_{Mn2})$ suitable for a linear three-spin (S_{Mn1}, S_{Fe1}, S_{Mn2} = 2, 1/2, 2) system has been used to fit the experimental data (6.5–300 K for complex **4**, and 5–300 K for complex **5**). The free Fe(III) anion was included as a constant term ($\chi_m T = (Ng^2\beta^2/3k)S_{Fe2}(S_{Fe2} + 1)$). Any intermolecular magnetic interaction was considered by using the molecular field approximation (zJ'). The best fit gave the parameters of J = –2.61(6) cm^{-1}, g = 2.00(1), zJ' = 0.17(1) cm^{-1}, and $R = \sum[(\chi_m T)_{calc} - (\chi_m T)_{obsd}]^2/\sum(\chi_m T)_{obsd}^2 = 3.1\times10^{-4}$ for complex **4**, and J = 3.72(6) cm^{-1}, g = 2.03(1), zJ' = 0.025(1) cm^{-1}, and $R = 4.4\times10^{-4}$ for complex **5** (solid lines in Fig. 5). The J values are comparable to that of the cyanide-bridged polynuclear Mn(III)–Fe(III) complexes.[6] The positive zJ' indicates the presence of noticeable global intermolecular ferromagnetic coupling.

 This journal is © The Royal Society of Chemistry 2009

View Online

Published on 23 February 2009 on http://pubs.rsc.org | doi:10.1039/B814860K
Downloaded by Xiamen University on 28 February 2011

Table 5 Comparison of the magnetic property of cyanide-bridged $Fe^{III}Mn^{III}$ complexes

compds	structure	Mn–N_{cyano} (Å)	C≡N–Mn (°)	magnetism	ref
$[Mn(salen)(EtOH)]_3[Fe(CN)_6]$	tetranuclear	2.249(2)–2.307(2)	170.7(2), 161.9(2), 148.9	AF AF F	13
[Mn(salcy)][Fe(mpzcq)$(CN)_3$]	1D	2.287(5), 2.298(5)	169.1(4), 154.3(5)	AF AF	16
$(NEt_4)[\{Mn(salen)\}_2Fe(CN)_6]$	2D	2.266(3) 2.337(3)	167.8(3) 146.2(2)	AF AF	23
1	dinuclear	2.256(3)	167.4(3)	F	This work
4	trinuclear	2.251(16) 2.154(14)	166.6(13) 162.7(12)	AF AF	This work
rac-(NEt_4)[Mn(salmen)(MeOH)]$_2$[Fe(CN)$_6$]	trinuclear	2.219(9)	164.7(9)	F	12
[Mn(salen)][Fe(mpzcq)$(CN)_3$]	dinuclear	2.275(3)	164.1(2)	AF	16
5	trinuclear	2.251(7) 2.207(7)	166.7(6) 158.3(7)	F F	This work
$[NEt_4]_2[Mn(saldmen)(H_2O)][Fe(CN)_6]$	dinuclear	2.198(9)	162.4(8)	F	24
$[Mn(salen)]_6[Fe(bpmb)(CN)_2]_6$	wheel	2.258(5)–2.354(4)	140.8(4)–163.3(5)	F	4
$[Mn(salen)]_6[Fe(bpClb)(CN)_2]_6$	wheel	2.250(4)–2.320(4)	138.4(4)–161.4(6)	F	5
$[Mn(salen)]_6[Fe(bpdmb)(CN)_2]_6$	wheel	2.234(7)–2.256(6)	141.6(5)–170.2(6)	F	5
$[Mn_2(5\text{-}Clsaltn)_2(H_2O)_2Fe(CN)_5(1\text{-}CH_3im)]$	trinuclear	2.221(5)–2.298(5)	165.2(6)–147.8(5)	F	26
$K[Mn(3\text{-}MeOsalen)]_2Fe(CN)_6$	2D	2.290(5) 2.415(5)	169.5(5) 137.2(4)	F F	18
$[Mn(salpn)(CH_3OH)]_4[Fe(CN)_6]ClO_4$	pentanuclear	2.261(3) 2.259(5)	160.2(3) 151.3(3)	F	14
$[Mn_2(5\text{-}Brsalen)_2Fe(CN)_5(1\text{-}CH_3im)]$	trinuclear	2.236(6), 2.222(6)	160.0(5), 154.3(5)	F	26
$[Mn_2(5\text{-}Clsaltmen)_2(H_2O)_2Fe(CN)_5(1\text{-}CH_3im)]$	trinuclear	2.311(3), 2.258(3)	159.7(3), 157.8(3)	F	26
$[Mn_2(5\text{-}Brsaltmen)_2(H_2O)_2Fe(CN)_5(1\text{-}CH_3im)]$	trinuclear	2.323(3), 2.266(3)	159.4(2), 157.2(3)	F	26
[Mn(salen)][Fe(bpb)$(CN)_2$]	1D	2.301(3), 2.439(3)	158.6(3), 151.8(3)	AF	4
[Mn(salen)][Fe(pzcq)$(CN)_3$]	1D	2.288(3), 2.263(3)	152.2(3), 158.3(3)	AF	15
$[Mn(5\text{-}Brsalpn)]_6[Fe(bpmb)(CN)_2]_6$	wheel	2.234(7), 2.256(6)	147.7(7), 158.2(6)	F	5
$[Mn(5\text{-}Clsalpn)]_6[Fe(bpmb)(CN)_2]_6$	wheel	2.236(4), 2.259(4)	145.8(4), 158.4(3)	F	5
$[Mn_4(saltmen)_4Fe(CN)_5(1\text{-}CH_3im)](ClO_4)_2$	2D	2.197(8)	157.3(7)	F	26
$[Mn_4(saltmen)_4Fe(CN)_6]ClO_4$	2D	2.19(1)	156.1(10)	F	18
$[NEt_4]_2[Mn(acacen)][Fe(CN)_6]$	1D	2.316(4)	156.2(3)	F	19
$[Mn(5\text{-}Clsalpn)]_2[Fe(bpmb)(CN)_2]_2$	tetranuclear	2.280(4)–2.349(3)	147.2(3)–155.4(3)	F	5
$Mn_3((R,R)\text{-}Salcy)_3(H_2O)_2Fe(CN)_6$	1D	2.398(4)–2.251(4)	143.0(3)–152.9(3)	AF	17
$K(18C6)(2\text{-}PrOH)_2\{Mn(acacen)\}_2\{Fe(CN)_6\}$	2D	2.331(3) 2.439(3)	152.0(3) 154.8(3)	F	24
$\{[Mn(salen)]_6[Fe(CN)_6]\}[Fe(CN)_6]$	heptanuclear	2.334(2)	150.74(14)	F	20
$Mn_2(5\text{-}Clsalen)_2(H_2O)_2Fe(CN)_5(1\text{-}CH_3im)]$	trinuclear	2.243(5)	149.8(5)	F	26
$\{Fe(CN)_4[CNMn(salen)(MeOH)]_2\}\{[Mn(salen)\text{-}(H_2O)]_2\}[Mn(salen)(H_2O)(MeOH)]_2[Fe(CN)_6]$	trinuclear	2.30(1)	149(1)	F	22
$(NEt_4)[Mn_2(salmen)_2(MeOH)_2Fe(CN)_6]$	1D	2.179(3)	146.7(4)	F	21
$(Et_4N)[Mn(acacen)Fe(CN)_5(1\text{-}CH_3im)]$	1D	2.331(4)	144.4(4)	AF	26
$K[(5\text{-}Brsalen)_2(H_2O)_2Mn_2Fe(CN)_6]$	trinuclear	2.331(5)	142.6(5)	F	25

pzcq$^-$ = 8-(pyrazine-2-carboxamido)quinoline, mpzcq$^-$ = 8-(5-methylpyrazine-2-carboxamido)quinoline anion, salcy^{2-} = *N,N′*-(trans-1,2-cyclohexanediylethylene)bis(salicylideneiminato) dianion, 1-CH_3im = 1-methylimidazole, acacen$^-$ = *N,N′*-ethylenebis(acetylacetonylideneaminato), salmen^{2-} = rac-*N,N′*-(1-methylethylene)bis(salicylideneiminate)), 18C6 = 18-crown-6-ether, saldmen^{2-} = *N,N′*-(1,1-dimethylethylene)bis(salicylideneiminato) dianion, rac-salmen^{2-} = rac-*N,N′*-(1-methylethylene)bis(salicylideneiminato) dianion.

Alternate-current (ac) magnetic susceptibility measurements for complexes **4** and **5** show the occurrence of frequency-dependent out-of-phase signals (inset of Fig. 5), indicative of the presence of slow relaxation of magnetization in both complexes.

The magnetic properties of complex **4** were further investigated by single crystal magnetic measurements made on a micro-SQUID.[10] The field dependence of magnetization at a sweep rate of 0.14 T s^{-1} clearly shows the occurrence of hysteresis below 0.5 K (ESI†, Fig. S8). At 0.04 K, the hysteresis loop exhibits a sigmoidal shape and only one QTM step at *ca.* zero magnetic field, as shown in Fig. 6. This suggests that complex **4** is an exchange-biased SMM because of the existence of intermolecular magnetic coupling. The very thin shape near zero magnetic field is a signature of the presence of intermolecular magnetic interaction. Similar behavior has been observed in other SMMs with weak intermolecular magnetic coupling.[5,11]

Magneto-structural correlationship. It has been experimentally shown that the magnetic coupling between low-spin Fe(III) and high-spin Mn(III) is ferromagnetic or antiferromagnetic because of the strict orthogonality of the magnetic orbitals ($[d_{xy}/d_{xz}/d_{yz}]^1$ in Fe^{III} *vs.* $d_{z^2}{}^1$ in Mn^{III}) and the orbital overlap between d_{xz}, d_{yz}, d_{xy} orbitals of Fe^{III} and Mn^{III}. The former effect contributes to ferromagnetic coupling, and the latter gives rise to antiferromagnetic interaction. Therefore, the overall magnetic property depends on which contribution is predominant. Table 5 collects the structure and magnetism of 36 cyanide-bridged Mn(III)–Fe(III) complexes.[4,5,12–26] In the complexes, the bridging cyanide nitrogen

View Online

Published on 23 February 2009 on http://pubs.rsc.org | doi:10.1039/B814860K
Downloaded by Xiamen University on 28 February 2011

atoms occupy the elongation axis of the octahedral coordination sphere of Mn(III), and the Mn–N_{cyano} bond distances are in the range 2.154(14)–2.439(3) Å. From Table 5, it can be found that the ferromagnetic property has been more frequently observed in cyanide-bridged Fe(III)–Mn(III) compounds, showing that the orbital orthogonality effect usually overwhelms the orbital overlap effect. It has been assumed that the magnetic interaction involved in the σ-type d_{z^2} orbital of Jahn–Teller Mn(III) makes a main contribution to the magnetic coupling.[27] Thus, ferromagnetic property occurs more frequently. However, the frequent bending of the Mn–N≡C–Fe linkages and the rotation of the *x* and *z* axes for Mn(III) should enlarge the overlap and therefore weaken the ferromagnetic contribution.[26] Close examination of the relation between C≡N–Mn bond angles and the magnetism in Table 5 shows that compounds with C≡N–Mn bond angles below 162° most probably exhibit ferromagnetic interaction with few exceptions, and above 162° both ferromagnetic and antiferromagnetic properties are possible.

Conclusions

Supramolecular assembly of polynuclear coordination compounds of *trans*-[Fe(*R*-bpb)$(CN)_2$]$^-$ has resulted in a series of novel molecular squares and macrocycles. The use of flexible Schiff base ligand 5-X-saltn^{2-} is responsible for the formation of polynuclear species. The Fe(III)–Mn(III) complex exhibits ferro- or antiferromagnetic interaction between Fe^{III} and Mn^{III} through cyanide bridges, whereas the hydrogen bonds between the non-bridging cyanide nitrogen atom and the solvent molecule (MeOH, EtOH or H_2O) transmit weak ferro- or antiferromagnetic coupling. The low-temperature single-crystal magnetic measurements for complex **4** show that it represents an additional example with exchange-biased SMM behavior because of the presence of appreciable intermolecular magnetic exchange. These results, along with our previous reports,[4,5] show that polynuclear compounds can be derived from the *trans*-[Fe(*R*-bpb)$(CN)_2$]$^-$. Future work will involve the synthesis of 1D Fe(III)–Mn(III) complexes based on *trans*-[Fe(X-bpb)$(CN)_2$]$^-$ and Mn(III)–Schiff bases, and single-chain magnets (SCMs) can be anticipated.

Acknowledgements

This work was supported by the Natural Science Foundation of China (project No.: 20671055 and 50873053) and Program for New Century Excellent Talents in University.

Notes and references

1 D. Gatteschi and R. Sessoli, *Angew. Chem. Int. Ed.*, 2003, **42**, 268; L. M. C. Beltran and J. R. Long, *Acc. Chem. Res.*, 2005, **38**, 325; J.-N. Rebilly and T. Mallah, *Struct. Bond*, 2006, **122**, 103; E. K. Brechin, *Chem. Commun.*, 2005, 5141; G. Aromi and E. K. Brechin, *Struct. Bond.*, 2006, **112**, 1.
2 F. Torres, J. M. Hernandez, X. Bohigas and J. Tejada, *Appl. Phys. Lett.*, 2000, **77**, 3248; R. Bircher, G. Chaboussant, C. Dobe, H. U. Güdel, S. T. Ochsenbein, A. Sieber and O. Waldmann, *Adv. Funct. Mater.*, 2006, **16**, 209.
3 H. Miyasaka and M Yamashita, *Dalton Trans.*, 2007, 399, and references therein.Wernsdorfer, N. Aliaga-Alcalde, D. N. Hendrickson and G. Christou, *Nature*, 2002, **416**, 406; K. C. Mondal, M. G. B. Drew and P. S. Mukherjee, *Inorg. Chem.*, 2007, **46**, 5625; E. E. Moushi, T. C. Stamatatos, W. Wernsdorfer, V. Nastopoulos, G. Christou and A. J. Tasiopoulos, *Angew. Chem. Int. Ed.*, 2006, **45**, 7722; L. Lecren, W. Wernsdorfer, Y.-G. Li, A. Vindigni, H. Miyasaka and R. Clerac, *J. Am. Chem. Soc.*, 2007, **129**, 5045; R. Bagai, W. Wernsdorfer, K. A. Abboud and G. Christou, *J. Am. Chem. Soc.*, 2007, **129**, 12918.
4 Z.-H. Ni, H.-Z. Kou, L.-F. Zhang, C. Ge, A.-L. Cui, R.-J. Wang, Y. Li and O. Sato, *Angew. Chem. Int. Ed.*, 2005, **44**, 7742.
5 Z.-H. Ni, L.-F. Zhang, V. Tangoulis, W. Wernsdorfer, A.-L. Cui, O. Sato and H.-Z. Kou, *Inorg. Chem.*, 2007, **46**, 6029.
6 D. J. Barnes, R. L. Chapman, R. S. Vagg and E. C. Watton, *J. Chem. Eng. Data*, 1978, **23**, 349–350.
7 (*a*) M. Ray, R. Mukherjee, J. F. Richardson and R. M. Buchanan, *J. Chem. Soc. Dalton Trans.*, 1993, 2451–2457; (*b*) S. K. Dutta, U. Beckmann, E. Bill, T. Weyhermuller and K. Wieghardt, *Inorg. Chem.*, 2000, **39**, 3355.
8 Z.-H. Ni, L. Zheng, L.-F. Zhang, A.-L. Cui, W.-W. Ni, C.-C. Zhao and H.-Z. Kou, *Eur. J. Inorg. Chem.*, 2007, 1240; P. Przychodzeń, K. Lewinski, M. Balanda, R. Pełka, M. Rams, T. Wasiutynshi, C. Guyard-Duhayon and B. Sieklucka, *Inorg. Chem.*, 2004, **43**, 2967.
9 S. L. Lambert, C. L. Spiro, R. R. Gagne and D. N. Hendrickson, *Inorg. Chem*, 1982, **21**, 68.
10 W. Wernsdorfer, *Adv. Chem. Phys.*, 2001, **118**, 99.
11 C. Boskovic, R. Bircher, P. L. W. Tregenna-Piggott, H. U. Gudel, C. Paulsen, W. Wernsdorfer, A.-L. Barra, E. Khatsko, A. Neels and H. Stoeckli-Evans, *J. Am. Chem. Soc.*, 2003, **125**, 14046; S. J. Langley, M. Helliwell, R. Sessoli, P. Rosa, W. Wernsdorfer and R. E. P. Weinpenny, *Chem. Commun.*, 2005, 5029.
12 H. Miyasaka, H. Ieda, N. Matsumoto, N. Re, R. Crescenzi and C. Floriani, *Inorg. Chem.*, 1998, **37**, 255.
13 H. Miyasaka, H. Takahashi, T. Madanbashi, K.-i. Sugiura, R. Clerac and H. Nojiri, *Inorg. Chem.*, 2005, **44**, 5969.
14 S.-F. Si, J.-K. Tang, Z.-Q. Liu, D.-Z. Liao, Z.-H. Jiang, S.-P. Yan and P. Cheng, *Inorg. Chem. Commun.*, 2003, **6**, 1109.
15 J. I. Kim, H. S. Yoo, E. K. Koh, H. C. Kim and C. S. Hong, *Inorg. Chem.*, 2007, **46**, 8481.
16 J. I. Kim, H. S. Yoo, E. K. Koh and C. S. Hong, *Inorg. Chem.*, 2007, **46**, 10461.
17 H.-R. Wen, C.-F. Wang, Y.-Z. Li, J.-L. Zuo, Y. Song and X.-Z. You, *Inorg. Chem.*, 2006, **45**, 7032.
18 H. Miyasaka, N. Matsumoto, H. Okawa, N. Re, E. Gallo and C. Floriani, *J. Am. Chem. Soc.*, 1996, **118**, 981.
19 N. Re, E. Gallo, C. Floriani, H. Miyasaka and N. Matsumoto, *Inorg. Chem.*, 1996, **35**, 6004.
20 X. Shen, B. Li, J. Zou, H. Hu and Z. Xu, *J. Mol. Struct.*, 2003, **657**, 325.
21 M. Ferbinteanu, H. Miyasaka, W. Wernsdorfer, K. Nakata, K.-i. Sugiura, M. Yamashita, C. Coulon and R. Clerac, *J. Am. Chem. Soc.*, 2005, **127**, 3090.
22 H. J. Choi, J. J. Sokol and J. R. Long, *J. Phys. Chem. Solids*, 2004, **65**, 839.
23 H. Miyasaka, H. Ieda, N. Matsumoto, K.-i. Sugiura and M. Yamashita, *Inorg. Chem.*, 2003, **42**, 3509.
24 H. Miyasaka, H. Okawa, A. Miyazaki and T. Enoki, *Inorg. Chem.*, 1998, **37**, 4878.
25 H. J. Choi, J. J. Sokol and J. R. Long, *Inorg. Chem.*, 2004, **43**, 1606.
26 W.-W. Ni, Z.-H. Ni, A.-L. Cui, X. Liang and H.-Z. Kou, *Inorg. Chem.*, 2007, **46**, 22.
27 K. R. Reddy, M. V. Rajasekharan and J.-P. Tuchagues, *Inorg. Chem.*, 1998, **37**, 5978.

 This journal is © The Royal Society of Chemistry 2009